

See discussions, stats, and author profiles for this publication at: <https://www.researchgate.net/publication/231643691>

Mechanistic Study on Hydrogen Spillover onto Graphitic Carbon Materials

ARTICLE *in* THE JOURNAL OF PHYSICAL CHEMISTRY C · NOVEMBER 2007

Impact Factor: 4.77 · DOI: 10.1021/jp074920g

CITATIONS

117

READS

21

4 AUTHORS, INCLUDING:



Liang Chen

National University of Defense Technology

110 PUBLICATIONS 1,383 CITATIONS

SEE PROFILE



Alan C. Cooper

Air Products and Chemicals

44 PUBLICATIONS 1,228 CITATIONS

SEE PROFILE



Hansong Cheng

China University of Geosciences

166 PUBLICATIONS 2,408 CITATIONS

SEE PROFILE

Mechanistic Study on Hydrogen Spillover onto Graphitic Carbon Materials

Liang Chen, Alan C. Cooper, Guido P. Pez, and Hansong Cheng*

Air Products and Chemicals, Incorporated, 7201 Hamilton Boulevard, Allentown, Pennsylvania 18195-1501

Received: June 24, 2007; In Final Form: September 25, 2007

We present a systematic study on the possible mechanisms of hydrogen spillover onto several carbon-based materials using density functional theory (DFT). Adsorption and diffusion of atomic hydrogen on a graphene sheet, single-walled carbon nanotubes, and a polyaromatic compound, hexabenzocoronene, were calculated, and the potential energies along the selected adsorption and diffusion minimum energy pathways were mapped out. We show that the migration of H atoms from a Pt cluster catalyst to the substrates is facile at ambient conditions with a small energy barrier, although the process is slightly endothermic, and that the H atoms can be either physisorbed or chemisorbed on carbon surfaces. Our results indicate that diffusion of H atoms in a chemisorbed state is energetically difficult since it requires C–H bond breaking and hydrogen spillover would occur likely via physisorption of H atoms. The curvature of the carbon materials is found to have a pronounced influence on the mobility of H atoms. The role of the “bridge” materials used in experiments is also discussed.

I. Introduction

Hydrogen adsorption in a variety of carbon materials, such as graphite and carbon nanotubes, has been widely studied both experimentally and theoretically due to their potential applications as storage media.^{1–4} Recent studies by Yang and co-workers have shown that a significant hydrogen storage capacity at ambient conditions can be achieved for several carbon-based materials via a hydrogen “spillover” process. It was hypothesized that in the “spillover” process a flux of atomic hydrogen, generated via dissociative chemisorption of molecular hydrogen upon interacting with platinum catalysts, first flows onto the carbon-based materials in the vicinity of catalytic particles through a “bridge” built with carbonized sugar molecules and then continues diffusing throughout the substrates.^{5,6} Since these carbon-based materials possess unsaturated bonds resulting from sp² carbons, it was deemed that the H adsorption and subsequent diffusion of atomic hydrogen on the substrates would ultimately lead to the formation of C–H bonds. The platinum catalyst acts as a source of hydrogen atoms derived from dissociative chemisorption of molecular hydrogen. The role of the “bridge” materials was supposed to bind the catalyst particles together with the receptor surfaces and to allow the hydrogen atoms to pass through to reach the surface, which then further diffuse throughout the entire receptor.⁵ The chemisorption energies of atomic hydrogen on graphite and single-walled carbon nanotubes (SWNTs) were reported to be in the range of 50–70 kcal/mol,^{7–9} which is 1 order of magnitude higher than the physisorption energy of molecular hydrogen in these materials.^{10,11}

To adequately address the spillover mechanism on graphitic materials, it is critical to understand the entire spillover processes including the chemical and transport behavior of the H atoms adsorbed. Yang and co-workers have studied atomic hydrogen adsorption on several selected SWNTs at very low occupancy using a molecular mechanics/quantum mechanics (MM/QM) method.^{8,12} Their results demonstrated the presence of multiple binding sites available for the spillover H on SWNTs. Sha and

co-workers have studied the structural and energetic properties of H atoms at one-eighth of a monolayer coverage on a graphite (0001) surface.^{7,13} They also calculated the potential energy surface on the graphite and attempted to address the H–H recombination dynamics. Hornekar et al. have studied the mechanism of hydrogen recombination on the graphite surface using temperature-programmed desorption (TPD) and density functional theory (DFT) methods.⁹ They reported that two hydrogen atoms adsorbed on the opposite sides of the graphite hexagon can recombine and desorb from the surface with a barrier of 1.4 eV. Lee et al.¹⁴ have investigated hydrogen adsorption and storage mechanisms in carbon nanotubes using DFT methods and proposed a flip-in and kick-in mechanism by which hydrogen atoms can be stored in the SWNT endohedral (interior) sites. Despite the abundant theoretical and experimental studies to date, the detailed mechanisms of hydrogen spillover on carbon-based materials is still poorly understood since these studies have only addressed a few selected steps of the spillover processes. In particular, it remains a mystery how a hydrogen atom coming from the “bridge” supported metal catalysts ultimately forms a C–H bond far from the vicinity of the catalyst particles. Obviously, in order for the spillover process to take place, two processes need to occur: (1) H atoms migrate from the catalyst to the substrate via chemisorption or physisorption; (2) H atoms diffuse from the adsorption sites at the vicinity of the catalyst to the sites far away from the catalyst.

In the present work, we attempt to address the entire spillover process theoretically by mapping out the energetics required for hydrogen atoms to flow onto the graphitic carbon surfaces proximal to a platinum catalyst subnanoparticle and subsequently to diffuse to other sites of the materials. To simplify the description of spillover on the graphitic materials, we used a small platinum cluster, Pt₆, to represent the catalyst particle. Small metal clusters have been widely used as a model of catalyst nanoparticles, and many studies have shown that the cluster models can provide useful insight into catalytic reaction processes.^{15–17} Molecular hydrogen undergoes a dissociative chemisorption process upon interacting with the cluster. Under

* Corresponding author. E-mail: chengh@airproducts.com.

a typical catalytic condition, the Pt cluster is fully saturated with hydrogen atoms with a threshold H desorption energy of approximately 2.4 eV.¹⁸ The carbon-based materials serving as the spillover substrates selected in the present study include a single graphene sheet, single-walled carbon nanotubes, and a finite aromatic molecule, hexabenzocoronene. The “bridge” utilized in the experimental study by Yang et al. was not incorporated in the theoretical model since its exact composition and structure in the systems are unknown. However, the possible role of the “bridge” in the spillover processes will be discussed.

To assist in our understanding of the hydrogen spillover mechanisms in carbon-based materials, we have recently undertaken a systematic study on hydrogen spillover mechanisms in a well-known hydrogen bronze spillover system, MoO₃.¹⁹ Despite extensive experimental and a few theoretical studies on the hydrogen bronze spillover systems, such as MoO₃ and WO₃, the underlying mechanism remained poorly understood. We found that the spillover process is largely dictated by the hydrogen-bonding network intrinsic to this type of material. The similar computational procedure was also utilized in the present study.

This paper is organized as follows. In section II, we outline the computational method used in the present study. The results and discussions are presented in section III. We first address how H atoms flow from Pt subnanoparticles by computing the reaction energy and the activation barrier. We then systematically examine the adsorption energies of H atoms on the selected substrates at various adsorption sites. In principle, the H atoms can undergo both physisorption and chemisorption processes on the substrate, largely depending on how “cold” the atoms are. If the atoms are sufficiently “cold” (i.e., have relative low kinetic energy), they can be physisorbed on the substrates due to a small energy barrier arising from the C–H bond formation. Otherwise, they will form C–H bonds with the graphitic C atoms. Finally, we explore the possible H atom diffusion pathways on the substrates. The implications to hydrogen spillover mechanisms and conclusions that can be derived from the present study are summarized in section IV.

II. Computational Method

All calculations were performed using DFT under the generalized gradient approximation with the exchange–correlation functional proposed by Perdew–Wang (PW91).^{20,21} The spin polarization scheme was utilized to deal with the electronically open-shell system. The electron–ion interactions were described by the projector augmented wave (PAW) pseudopotentials.²² An energy cutoff of 400 eV was used to make sure that the total energy is well converged. All atoms were fully relaxed with the energy converged to less than 10^{−4} eV. The computational method is implemented in the Vienna ab initio simulation package (VASP).^{23,24}

A symmetric slab supercell containing one (5 × 5) graphene sheet and 16 Å vacuum space was used to model the graphite (0001) surface. The supercell contained 50 carbon atoms, with a dimension of 12.2 Å × 12.2 Å × 16 Å. The adsorption of H on the SWNTs was simulated in a rectangular supercell containing one isolated SWNT tube with two primitive unit cells. The size of the supercell is 20 Å × 20 Å × 7.4 Å. A hexabenzocoronene molecule is placed in the center of a 20 Å × 20 Å × 20 Å box. The Brillouin zone was sampled with 2 × 2 × 1 and 1 × 1 × 2 Monkhorst–Pack meshes for graphite and SWNTs,²⁵ respectively, and only with a Γ -point for hexabenzocoronene. In all the above models, periodic boundary conditions were imposed. For the finite aromatic system, the

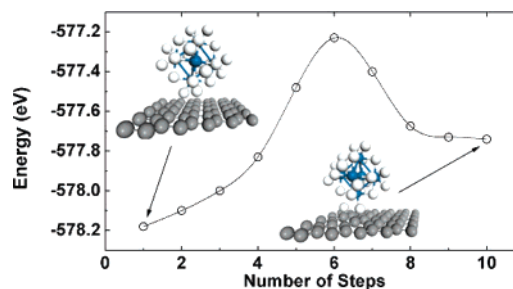


Figure 1. Spillover of hydrogen from Pt₆ (upper inset) to the graphene sheet (lower inset). The line is drawn as a guide to the eye.

selected box size is large enough so that the closest atomic distance between two adjacent boxes is larger than 8.0 Å. The nudged elastic band (NEB) method^{26,27} was used to determine the minimum energy pathways for H diffusion. Initial and final states were selected based on the adsorption calculations, and the number of images was chosen to derive smooth potential energy curves. The adsorption energy of a H atom is defined as

$$\Delta E = E(\text{H}) + E(\text{substrate}) - E(\text{H} + \text{substrate}) \quad (1)$$

where $E(\text{H})$, $E(\text{substrate})$, and $E(\text{H} + \text{substrate})$ represent the energies of a single H atom in the gas phase, the substrate, and the substrate with adsorbed H atom, respectively.

III. Results and Discussion

III.A. H Migration from Catalyst to a Graphene Sheet.

To simplify the calculations, we first represent the Pt catalyst with a subnanocluster, Pt₆. The cluster is obviously much smaller than the catalyst particles used in experiments. However, when used in the study of catalyst–substrate interface, it can yield useful physical insight into the catalytic reaction processes. A recent study by Zhou et al. suggests that some of the important properties, such as H₂ dissociative chemisorption and H desorption energies at full cluster saturation with H atoms, do not change significantly with the cluster size.²⁸ Under a typical catalytic condition, Pt clusters are fully covered by H atoms. We have identified in a previous study on the dissociative chemisorption of H₂ on Pt₆ that the desorption energy of a H atom at full cluster coverage (Pt/H = 1:4) is 2.44 eV,¹⁸ which is the minimum energy required for a H atom to dissociate from the Pt catalyst. The high desorption energy is to be expected due to lack of a H acceptor, except that the atom could undergo a recombination process with another H to form a H₂ molecule, which is irrelevant for the catalytic process of our current interest despite being facile at full H coverage.

We next performed minimum energy pathway calculations by gradually moving the fully saturated Pt₆ cluster, which has a composition of Pt₆H₂₄, toward the graphene sheet. Except for the designated reaction coordinate, defined by the vertical distance between the center of mass of the fully saturated Pt₆ cluster and a single carbon atom of the graphene sheet, all other degrees of freedom were allowed to relax. It is understood that the metal hydride is formed upon adsorption of the Pt₆ cluster on graphene in real systems. However, we found that the H migration barrier in this case does not change significantly from the one obtained from the minimum energy pathway calculations. The calculated potential energy curve is shown in Figure 1. Indeed, the process results in migration of two H atoms from the catalyst to the graphene sheet to form two C–H bonds and is slightly thermodynamically endothermic with an average reaction energy of 0.23 eV per H atom. In contrast to the high

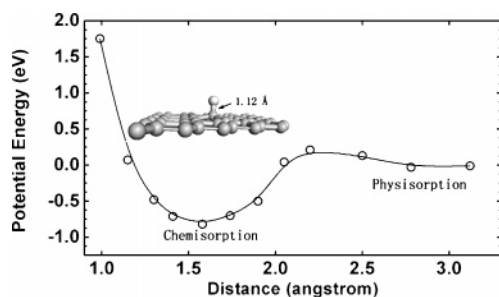


Figure 2. Potential energy curve for hydrogen adsorbed on top of carbon atoms in a graphene sheet vs the distance between H and the surface.

H desorption energy in the fully saturated Pt_6 cluster, the calculated average activation barrier for the migration is 0.48 eV per H atom, indicating that the process is kinetically facile as well. The results suggest that H migration from Pt catalyst to graphene sheet at the vicinity of the catalyst can occur at ambient conditions.

The above calculation suggests that direct contact between the fully saturated Pt cluster and the graphene sheet can result in C–H bond formation. In the experiments conducted by Yang and co-workers, the Pt catalyst nanoparticles are dispersed on a support with intermediate bridge material made of carbonized sugar. These materials may prevent the catalyst particles from coming into direct contact with the substrate. It was speculated that H atoms can still come out of the catalyst and pass through the surfaces of the support and bridge to enter the substrate surfaces.⁵ Depending on how energetic these H atoms are, they may interact with the surfaces via a chemisorption or a physisorption process. Figure 2 displays the calculated potential energy curve for a H atom to approach a graphene sheet from a large distance to form a C–H bond. Indeed, starting at the distance of approximately 2.5 Å, the potential energy becomes slightly repulsive until around 2.2 Å, after which the energy decreases rapidly. The calculated energy barrier is about 0.2 eV, which agrees with the value reported by Sha and Jackson.⁷ Detailed structural examination reveals that the repulsion arises from the fact that the C atom must come out of the graphene plane in order to form a C–H bond with the incoming H atom, which imposes strain on the neighboring C atoms. Therefore, if the H atoms coming out of the catalyst become sufficiently “cold” after moving across the surfaces of support and/or bridge material, it is possible that they can be blocked from immediate formation of a C–H bond by the energy barrier and thus be physisorbed on the substrate surface. The calculated physisorption energy on the graphite and SWNTs for the H atom is less than 0.1 eV. On the other hand, if the H atoms are “hot”, they can easily overcome the barrier to form C–H bonds with the graphitic C atoms.

A key issue concerning the mechanism of hydrogen spillover, therefore, is whether the H atoms, regardless of physisorption or chemisorption, would diffuse throughout the substrates.

We will first examine the situation of chemisorption, which leads to C–H bond formation, in several graphitic materials. The systems selected in our calculation are a graphene sheet, two armchair single-walled carbon nanotubes (SWNTs), (5,5) and (9,9), and a finite aromatic molecule, hexabenzocoronene.

III.B. H Adsorption. For graphene and SWNTs, H is found to be chemisorbed directly above the carbon atom, with the optimized C–H bond length in the range of 1.10–1.12 Å. No binding states are identified above the center of the hexagon, as expected. The calculated chemisorption energies of H on graphene and the exterior of (9,9) and (5,5) SWNTs are 0.82,

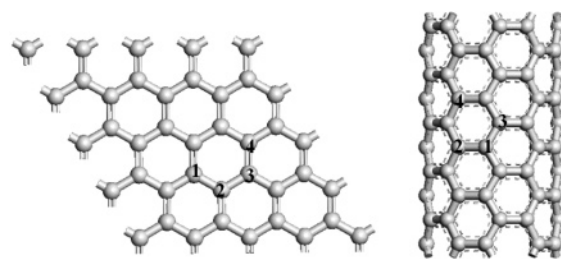


Figure 3. Hydrogen adsorption sites on a graphene sheet (left) and SWNT (right).

1.07, and 1.43 eV, respectively. The calculated H adsorption energy on graphene is consistent with what was reported by Sha and Jackson.⁷ H chemisorption on the (5,5) SWNT is the strongest among the three graphitic systems since carbon atoms tend to possess more character of sp^3 hybridization in SWNT with a smaller radius due to their higher curvature. The curvature effect on hydrogen and SWNTs interactions has been quantitatively addressed previously by Kostov et al.²⁹ Upon H chemisorption on the graphene sheet, the carbon atom underneath the adsorbed H is puckered up from the graphene plane by 0.05 Å as its hybridization changes from sp^2 to sp^3 . Consequently, the three adjacent C–C bond lengths are increased by 0.08–0.1 Å. For the SWNTs, the carbon atom that forms the C–H bond is pulled out of the plane of the nanotube wall slightly less, depending on the nanotube curvature, due to the preformed quasi- sp^3 -like hybridization of the carbon atoms. Our calculations give the desorption activation energies of H atom from graphene and (9,9) and (5,5) SWNTs of 1.03, 1.25, and 1.61 eV, respectively, reflecting the fact that H desorption requires compensation for not only the chemisorption energy but also the 0.2 eV barrier shown in Figure 2. It is also important to point out that the C–H bonds formed in the above materials at a low coverage are much weaker than those in small organic molecules largely due to the fact that the carbon atoms in the present cases are strained with a strong tendency to return to their original sp^2 configuration.

Next, we investigated the coadsorption of two H atoms on opposite sides of the graphene sheet. The results indicate that the average adsorption energy per H atom for forming two C–H bonds with adjacent carbon atoms of an alternative conformation (sites 1 and 2 in Figure 3) is 0.3 eV more favorable than with the two alternative carbon atoms (sites 1 and 3 in Figure 3). This can be easily understood by taking into account the change of hybridization. Upon the formation of the first C–H bond, the carbon atom underneath is pulled outward as its electronic configuration changes from sp^2 to sp^3 . Consequently, the three adjacent carbon atoms are slightly pushed inward to accommodate the quasi- sp^3 configuration. The new quasi- sp^3 -like carbon enhances the adsorption of the incoming second H on the opposite side. In contrast, for SWNTs, the coadsorption of two H atoms on opposite sides is not energetically favorable. The interaction of H on the interior wall of SWNTs is much weaker than on the exterior wall due to the curvature effect. As indicated in other ab initio calculations, the H atoms adsorbed in the interior sites can readily desorb at room temperature.⁸

For hexabenzocoronene, the C–H bond strength follows the trend that the closer the carbon atom is to the edge of the molecule, the stronger the C–H bond. This is because the C–H bond formation near the edge gives rise to much less structural strain upon loss of coplanarity with other carbon atoms, and thus the C–H bond is more stable. The calculated chemisorption energies for the selected C atoms are shown in Table 1.

TABLE 1: Calculated Chemisorption Energies of H on Selected Carbon Atoms

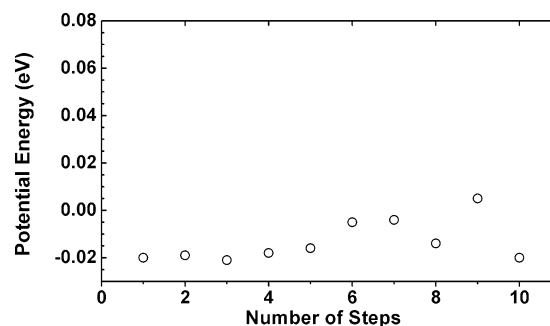
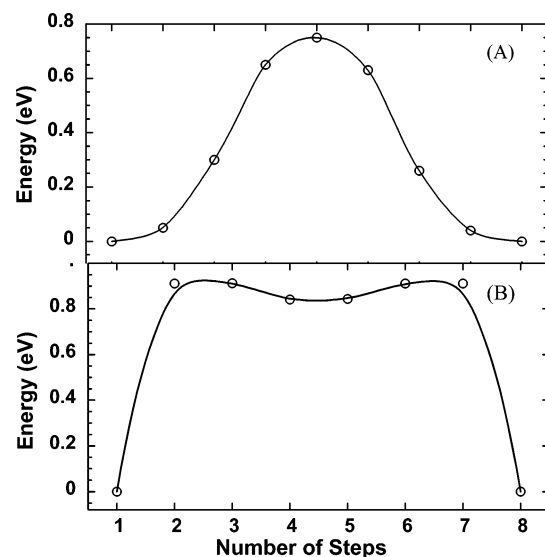
	graphene	(5,5) SWNT	(9,9) SWNT	hexabenzocoronene (site 1)
ΔE_{chem} (eV)	0.82	1.07	1.43	1.01

We now address the possibility of H physisorption on graphene. Figure 4 displays the potential energies in the physisorption region of C–H distances, i.e., about 2.5 Å above the graphene sheet. The calculated energies are rather flat, indicating a site-independent behavior. In other words, if the H atom is physisorbed on graphene, it can move across the plane with minimal energy changes. It is important to point out that H physisorption arising from the van der Waals force cannot be adequately described by DFT. Nevertheless, regardless of the computational methods used in the calculations, the adsorption energy is obviously very small, as qualitatively indicated in our results.

III.C. H Diffusion on Graphene. We now investigate the possible H diffusion routes on a graphene sheet, in which a C–H bond is formed, by calculating the minimum energy pathways. In Figure 4, we label the C atoms to which a H atom chemisorbed on site 1 would migrate. For simplicity, only the case in which there is only one C–H bond in the selected supercell was studied. It is anticipated that both the calculated reaction energies and activation barriers will be higher if more C–H bonds are involved since a higher number of C–H bonds with energetically favorable conformation would prevent the C–H bond dissociation and thus give rise to high activation barrier.

Figure 5A displays the calculated potential energy curve for a H atom to move from a C atom to an adjacent C atom (site 1 to site 2, as shown in Figure 4). The calculation yields an activation energy of 0.78 eV, which is close to the adsorption energy but slightly lower than the activation energy required to desorb from the surface. Clearly, this result indicates that the C–H bond needs to be broken in order for the H atom to move. This stringent requirement of course hinders the H diffusion. Upon H diffusion, the puckered carbon atom moves back toward its original lattice site. Simultaneously, the adjacent carbon atom is pulled out and thus forms a new C–H bond. For H diffusion from site 1 to site 3, the calculated minimum energy pathway indicates that the H atom must pass through site 2. Therefore, the calculated potential energy curve for the diffusion pathway is simply a duplicate of Figure 5A.

Figure 5B displays the calculated potential energy along the H diffusion pathway from site 1 to site 4 as shown in Figure 4. It exhibits a double-hump shape representing essentially three consecutive steps. First, H is desorbed from the surface. Second, H is adsorbed at a metastable site above the center of the hexagonal ring. Finally, H reaches its destination by forming a strong C–H bond at site 4. The rate-limiting step is the transition from the chemisorption state to the metastable site with a barrier of 0.95 eV, which is slightly higher than the activation energy of diffusion between two adjacent sites. Considering the small energy difference between diffusion pathways of 0.17 eV, it is likely that the two diffusion pathways may coexist at high temperatures. It was recently claimed by Ye and Chiu that atomic hydrogen is mobile on graphite at room temperature based on their observation in the experiment of graphite-mediated reduction of azoaromatic compounds with elementary iron in lialysis cells.³⁰ We suspect that they might have observed the hydrogen diffusion in the physisorption region. We have also investigated several possible diffusion routes of two H

**Figure 4.** Diffusion of hydrogen at physisorption C–H distances on a graphene sheet.**Figure 5.** H diffusion of chemisorbed hydrogen on a graphene sheet; the line is drawn as a guide to the eye. (A) Diffusion from site 1 to site 2. (B) Diffusion from site 1 to site 4.

atoms chemisorbed on opposite sides of two neighboring C atoms starting from the optimized coadsorption structure. It was found that even the lowest activation energy is larger than 1.5 eV. We thus conclude that the concerted motion of two H atoms is not energetically viable. Our results are consistent with the recent report using scanning tunneling microscopy and DFT calculations on diffusion of two separated H atoms on graphite (0001) surface which concluded that simultaneous diffusion of two H atoms is energetically unfavorable.⁹

III.D. H Diffusion on the Exterior Wall of (5,5) and (9,9) SWNTs. We next investigated the H diffusion on SWNTs following the longitudinal (from site 1 to 3 in Figure 4) and horizontal (from site 1 to 2) directions of (5,5) and (9,9) SWNTs. As shown in Figures 6 and 7, the energy profiles of diffusion pathways following the two different directions are virtually identical for both SWNTs. The three adjacent carbon atoms near the C–H bond are symmetrically placed; thus the H has the equal probability to diffuse onto any of them. Figures 6 and 7 show that the calculated diffusion activation energies are 1.42 and 1.09 eV on (5,5) and (9,9) SWNTs, respectively. These values are very close to the corresponding adsorption energies, which again indicates C–H bond breaking upon diffusion. Once again, the calculated energy profiles reflect the strong influence of the SWNT curvatures. A large curvature positively enhances the adsorption strength but also significantly reduces the mobility of H on the surface. When compared with the results on the graphene sheet, it is more difficult for the H atom to diffuse on sp³-like carbon atoms.

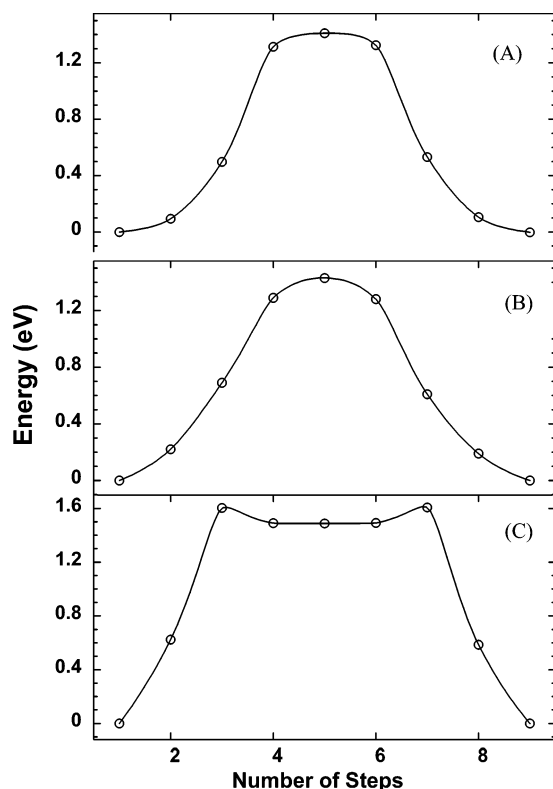


Figure 6. Calculated H diffusion pathway on the exterior wall of SWNT (5,5). (A) Diffusion from site 1 to site 2 (horizontal). (B) Diffusion from site 1 to site 3 (longitudinal). (C) Diffusion from site 1 to site 4.

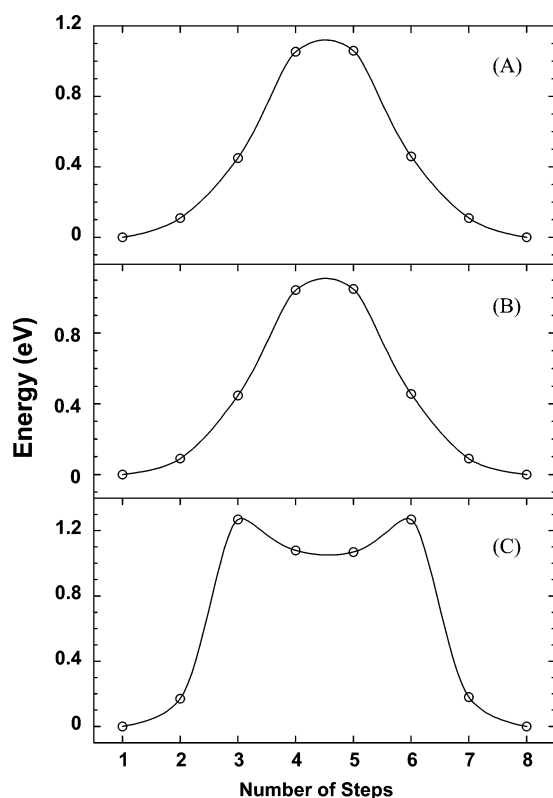


Figure 7. Calculated H diffusion pathway on the exterior wall of SWNT (9,9). (A) Diffusion from site 1 to site 2 (horizontal). (B) Diffusion from site 1 to site 3 (longitudinal). (C) Diffusion from site 1 to site 4.

Similar to H diffusion on the graphene sheet, the H diffusion from site 1 to 4 on SWNTs also consists of three steps. The

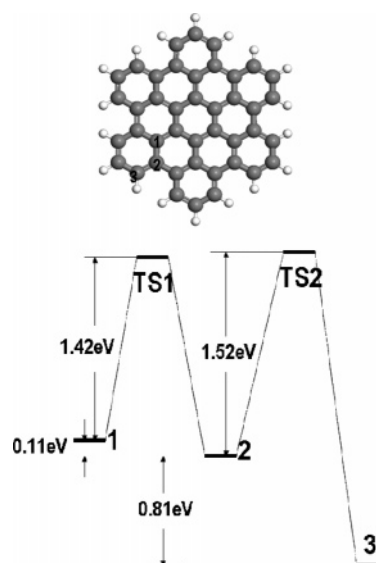


Figure 8. Schematic of hexabenzocoronene and energy landscape for H adsorption and diffusion.

rate-limiting step is still the first “desorption” step. The activation energies are 1.61 and 1.29 eV on (5,5) and (9,9) SWNTs, respectively. These results show that the H atoms are unlikely to diffuse freely at ambient temperatures and pressures. The curvature effect on the diffusion becomes more pronounced as the radii of the SWNTs get smaller.

III.E. H Diffusion on Hexabenzocoronene. Finally, we considered H diffusion from an inner site to the edge of hexabenzocoronene. The calculated energy landscape diagram of adsorption and transition states is presented in Figure 8. The calculated diffusion activation energies from site 1 to 2 and from site 2 to 3 are 1.52 and 1.42 eV, respectively. The activation energies are much higher than that for the graphene sheet but similar to that on the exterior wall of (5,5) SWNT. The diffusion is accompanied by considerable structural bending in order to accommodate the change of electronic configuration toward sp^3 hybridization. The bending as well as the diffusion on sp^3 carbons significantly increases the activation energy required. In contrast, H diffusion on the flat graphene sheet and exterior walls of SWNTs is rather local with a smaller extent of structural relaxation, in which only the H and the adjacent few carbon atoms are involved, due to their well-connected graphitic network.

IV. Summary

Hydrogen spillover onto carbon-based materials represents a novel technique to store hydrogen in a variety of materials that are readily available. Despite the fact that the concept of hydrogen spillover is not new, its applications to carbon-based materials are unprecedented. If a large storage capacity can be realized to help meet the hydrogen storage system targets set by the U.S. Department of Energy, the method could be potentially useful for large-scale applications. In this paper, we attempt to systematically address the fundamental mechanisms that govern the spillover processes in carbon-based materials using DFT.

To clearly describe the spillover processes, we selected three graphitic carbon materials representing both finite and extended systems. The catalyst was modeled with a Pt cluster fully saturated by H atoms. The effect of support and bridge materials was neglected in our theoretical model. The hydrogen spillover processes were then broken into three steps. The first step

involves H₂ dissociative chemisorption into H atoms on the Pt catalyst. We showed previously that this process is energetically favorable. In the second step, the Pt catalyst fully saturated by H atoms delivers H atoms to the graphitic surfaces. The migration of H atoms from the catalyst to the substrates may involve both chemisorption and physisorption processes. Our computational results indicate that the chemisorption process might be able to proceed readily at ambient conditions with small to moderate activation barriers. The calculated H chemisorption strength was found to be curvature-dependent with higher adsorption energies associated with the carbon atoms of nanotubes with more pronounced curvature. With the minimum H desorption energy of approximately 2.4 eV from the fully saturated Pt cluster, we speculate that the physisorption process could only be induced by the support and/or bridge materials. Our previous computational study on hydrogen spillover in MoO₃, which is a well-known spillover system, suggests that this process in a massive H-bonding system can readily take place. The bridge materials used in Yang's experimental studies are composed of carbonized sugar (e.g., sucrose) molecules. Although the material was carbonized upon heat treatment at 400 °C for several hours, oxygen atoms left over in the form of oxygen-containing functional groups could still be relevant for hydrogen spillover. It is possible that those oxygen atoms (likely, in the form of graphite oxides) provide a H-bonding network, similar to what was found in MoO₃, that allows H atoms on the Pt catalyst to migrate to the substrate. If these H atoms are "hot" upon migration, they will immediately form a bond with a carbon atom nearby. If they are sufficiently "cold", the H atoms will be physisorbed at least 2.5 Å above the graphitic surfaces, in which case H diffusion throughout the surfaces is energetically feasible. Of course, it remains a question how stable these physisorbed H atoms are on the carbon material surfaces and the degree to which H atoms recombine to form molecular hydrogen. Preliminary ab initio molecular dynamics simulation of 60 H atoms physisorbed on C₆₀ at room temperature suggests that most of the H atoms will either form C–H bonds with the fullerene or recombine to form H₂ molecules, the latter of which of course does not contribute to the overall hydrogen storage capacity. In the final step of the hydrogen spillover process, we studied diffusion of a H atom chemisorbed on surfaces of the selected graphitic materials. Similar to the calculated chemisorption strength, the calculated diffusion barriers were also found to be curvature-dependent with a higher barrier associated with carbon atoms of higher curvature SWNTs. Our computational results suggest that it would be difficult for chemisorbed H atoms to move freely at moderate, near-ambient temperatures since diffusion must require C–H bond dissociation, which requires a substantial activation energy for all the materials investigated here. We therefore conclude that H diffusion in the graphitic materials would not be energetically favorable if the H atom is chemisorbed and the most probable mechanism for H atoms to spread out in the entire materials is via physisorption.

An interesting question is how stable the physisorbed H atoms are on surfaces of the carbon materials. Our preliminary results

on collisions of physisorbed H atoms with C₆₀ at room temperature using ab initio molecular dynamics simulations suggest that these H atoms will readily recombine to form H₂ molecules or form C–H bonds with C₆₀ if they gain enough momentum.³¹ In other words, physisorbed H atoms have a limited lifetime in a stable, adsorbed state at a finite temperature.

The present work has not directly addressed the role of support and bridge materials. Full understanding of hydrogen spillover mechanisms would require incorporating the structure of these materials, especially the bridge material, into the theoretical model, which is a subject of active research.

Acknowledgment. The authors gratefully acknowledge funding for this work provided by the U.S. Department of Energy's Office of Energy Efficiency and Renewable Energy via the Hydrogen Sorption Center of Excellence.

References and Notes

- (1) Jeloica, L.; Sidis, V. *Chem. Phys. Lett.* **1999**, *300*, 157.
- (2) Ferro, Y.; Marinelli, F.; Allouche, A. *J. Chem. Phys.* **2002**, *116*, 8124.
- (3) Ferro, Y.; Marinelli, F.; Allouche, A. *Chem. Phys. Lett.* **2003**, *368*, 609.
- (4) Volpe, M.; Cleri, F. *Surf. Sci.* **2003**, *544*, 24.
- (5) Lachawiec, A. J.; Qi, G.; Yang, R. T. *Langmuir* **2005**, *21*, 11418.
- (6) Lueking, A. D.; Yang, R. T.; Baker, N. M. *Langmuir* **2004**, *20*, 714.
- (7) Sha, X.; Jackson, B. *Surf. Sci.* **2002**, *496*, 318.
- (8) Yang, F. H.; Lachawiec, A. J.; Yang, R. T. *J. Phys. Chem. B* **2006**, *110*, 6236.
- (9) Hornekar, L.; et al. *Phys. Rev. Lett.* **2006**, *96*, 156104.
- (10) Wang, Q.; Johnson, J. K. *J. Phys. Chem. B* **1999**, *103*, 4809.
- (11) Wang, Q.; Johnson, J. K. *Mol. Phys.* **1998**, *95*, 299.
- (12) Yang, F.; Yang, R. T. *Carbon* **2002**, *40*, 437.
- (13) Zecho, T.; Guttler, A.; Sha, X.; Jackson, B.; Kupperts, J. *J. Chem. Phys.* **2002**, *117*, 8486.
- (14) Lee, S. M.; An, K. H.; Lee, Y. H.; Seifert, G.; Frauenheim, T. *J. Am. Chem. Soc.* **2001**, *123*, 5059.
- (15) Du, A. J.; Smith, S. C.; Yao, X. D.; Lu, G. Q. *J. Am. Chem. Soc.* **2007**, *129*, 10201.
- (16) Ivanova Shor, E. A.; Nasluzov, V. A.; Shor, A. M.; Vayssilov, G. N.; Rosch, N. *J. Phys. Chem. C* **2007**, *111*, 12340.
- (17) Jung, C.; Tsuboi, H.; Koyama, M.; Kubo, M.; Broclawik, E.; Miyamoto, A. *Catal. Today* **2006**, *111*, 322.
- (18) Chen, L.; Cooper, A. C.; Pez, G. P.; Cheng, H. *J. Phys. Chem. C* **2007**, *111*, 5514.
- (19) Chen, L.; Pez, G. P.; Cheng, H. *Phys. Rev. Lett.*, submitted for publication.
- (20) Perdew, J. P.; Chevary, J. A.; Vosco, S. H.; Jackson, K. A.; Pederson, M. R.; Singh, D. J.; Fiolhais, C. *Phys. Rev. B* **1992**, *46*, 6671.
- (21) Blochl, P. E. *Phys. Rev. B* **1994**, *50*, 17953.
- (22) Kresse, G.; Joubert, J. *Phys. Rev. B* **1999**, *59*, 1758.
- (23) Kresse, G.; Hafner, J. *Phys. Rev. B* **1993**, *48*, 13115.
- (24) Kresse, G.; Furthmüller, J. *Comput. Mater. Sci.* **1996**, *6*, 15.
- (25) Monkhorst, H. J.; Pack, J. D. *Phys. Rev. B* **1976**, *13*, 5188.
- (26) Mills, G.; Jónsson, H.; Schenter, G. K. *Surf. Sci.* **1995**, *324*, 305.
- (27) Jónsson, H.; Mills, G.; Jacobsen, K. W. Nudged Elastic Band Method for Finding Minimum Energy Paths of Transitions. In *Classical and Quantum Dynamics in Condensed Phase Simulations*; Berne, B. J., Ciccotti, G., Coker, D. F., Eds.; World Scientific: River Edge, NJ, 1998.
- (28) Zhou, C.; Wu, J.; Nie, A.; Forrey, R. C.; Tachibana, A.; Cheng, H. *J. Phys. Chem. C*, submitted for publication.
- (29) Kostov, M. K.; Cheng, H.; Cooper, A. C.; Pez, G. P. *Phys. Rev. Lett.* **2002**, *89*, 146105.
- (30) Ye, J.; Chiu, P. *Environ. Sci. Technol.* **2006**, *40*, 3959.
- (31) Knippenburg, M. T.; Cheng, H. To be submitted for publication.